Crystal Structures, Thermal Behaviors, and C−H···O═C Hydrogen Bondings of Poly(3-hydroxyvalerate) and Poly(3-hydroxybutyrate) Studied by Infrared Spectroscopy and X-ray Diffraction

Harumi Sato,*,†,‡ Yuriko Ando,†,‡ Jiří Dybal,‡,§ Tadahisa Iwata,‡,∥ Isao Noda,‡,⊥ and Yukihiro Ozaki†,‡

School of Science and Technology and Research Center for Environment Friendly Polymers, Kwansei-Gakuin University, Sanda 669-1337, Japan; Institute of Macromolecular Chemistry, Academy of Science of the Czech Republic, Prague, Czech Republic; Department of Biomaterial Sciences, Graduate School of Agricultural and Life Sciences, The University of Tokyo, Yayoi, Bunkyo-ku, Tokyo 113-8657, Japan; and The Procter & Gamble Company, 8611 Beckett Road, West Chester, Ohio 45069

Received October 4, 2007; Revised Manuscript Received March 27, 2008

ABSTRACT: We have investigated crystal structure and C−H···O═C hydrogen bonding by using infrared (IR) spectroscopy and wide-angle X-ray diffraction (WAXD) for poly(3-hydroxyvalerate) (PHV) in comparison with those of poly(3-hydroxybutyrate) (PHB). We have explored the distances between the C═O group in one helix and the CH_3 or CH_2 groups in the other helix of PHV by using X-ray crystallographic data. It has turned out that the distance between the C═O group and the CH_3 group of PHV is longer than that of the van der Waals separation (2.72 Å), while the distance between the C═O group and the two CH_2 groups in the main and side chains of PHV is significantly shorter than that of the van der Waals separation. Therefore, it is very likely that PHV has C−H···O═C hydrogen bondings between the C═O group and the one or two CH_2 groups in the main or side chains. Of particular note is that CH_2 antisymmetric and symmetric stretching bands of PHV show large blue shifts, which are characteristic of C−H···O hydrogen bondings. These strongly support the existence of CH_2···O═C hydrogen bondings in PHV. PHV shows three crystalline C═O stretching bands at 1740, 1725, and 1721 cm^{-1}, suggesting that the C═O groups are in three different environments in the PHV crystal. The frequencies of the 1725 and 1721 cm^{-1} bands are very close to that of the crystalline C═O stretching band of PHB (1723 cm^{-1}). We have assigned these two C═O stretching bands of PHV to the C═O group that has hydrogen bonds with both side chain and main chain CH_2 groups and that has a hydrogen bond with one of the CH_2 groups. Temperature-dependent increases in the *a* and *b* lattice parameters of PHV indicate that the directions of C−H···O═C hydrogen bondings are almost in parallel to the (110) diffraction, which is the chain folding direction of PHV. PHB has a particular C−H···O═C hydrogen bonding between the C═O group and the CH_3 group along the *a* axis ((110) to (1$\bar{1}$0) direction), which is the same direction as its chain folding direction. The difference in the chain folding direction between PHV and PHB may come from the difference in the inter- or intramolecular interactions in their crystal structures.

Introduction

Polyhydroxyalkanoate (PHA) polymers are optically active aliphatic polyesters produced by bacterial fermentation and have the biodegradability. Among all the natural polymers, PHA polymers possess thermoplasticity and mechanical properties similar to those of synthetic polymers.[1,2] Thus, many research groups have been involved in developing PHAs with desirable physical properties. Poly(3-hydroxybutyrate) (PHB) is a typical polymer of the PHA group. PHB is highly crystalline and hence too rigid, stiff, and brittle.[3–10] Poly(3-hydroxyvalerate) (PHV) also belongs to the PHA family. Figure 1 compares chemical and crystal structures of PHV and PHB. These chemical structures are very similar to each other; PHB has a methyl side chain, while PHV has an ethyl side chain. Both PHV and PHB have orthorhombic, $P2_12_12_1$ unit cell with lattice parameters of $a = 9.32$ Å, $b = 10.02$ Å, and $c = 5.56$ Å[11,12] and $a = 5.76$ Å, $b = 13.20$ Å, and $c = 5.96$ Å,[13,14] respectively (Figure 1). Though their helical structures are very similar, the chain-folding directions are different; growth planes of PHB single crystals are {100} (along the *a* axis)[15,16] while those of PHV are the {110} direction.[17] Recently, on the basis of molecular weight studies on depolymerase-treated single crystals of PHB, Marchessault et al.[15,16] suggested that the PHB single crystals create a multiple erosion surface in the fold plane direction, i.e., parallel to the long axis of the lamella (*a* axis of unit cell). On the other hand, the growth planes of PHV single crystals are {110}, and the average direction of chain folding determined by polyethylene decoration is in parallel to these growth planes.[17]

In our previous IR and WAXD studies of PHB,[18–23] we found that PHB has the C−H···O═C hydrogen bonding between the C═O group in one helix and the CH_3 group in the other helix along the *a* axis. Evidences for proposing the C−H···O═C hydrogen bonding in PHB came from the following facts: (1) a C−H stretching band appears at above 3000 cm^{-1}, an unusually high frequency, and the corresponding C═O stretching band shows a low-frequency shift; (2) the distance between the O atom of the C═O group and the H atom of one of the C−H bonds of the CH_3 group is shorter than that of the van der Waals separation (2.72 Å); (3) quantum chemical calculation of dimer model compounds of PHB revealed that the molecular structure with a C−H···O═C hydrogen bonding is the most stable structure. One of the most important findings of our previous PHB studies is that the direction of the hydrogen bonding is almost parallel to the direction of the chain folding lamella structure. In PHB the chain folding is alternating

* To whom all correspondence should be addressed. E-mail: hsato@kwansei.ac.jp.
† School of Science and Technology, Kwansei-Gakuin University.
‡ Research Center for Environment Friendly Polymers, Kwansei-Gakuin University.
§ Academy of Science of the Czech Republic.
∥ The University of Tokyo.
⊥ The Procter & Gamble Company.

10.1021/ma702222a CCC: $40.75
Published on Web 05/21/2008

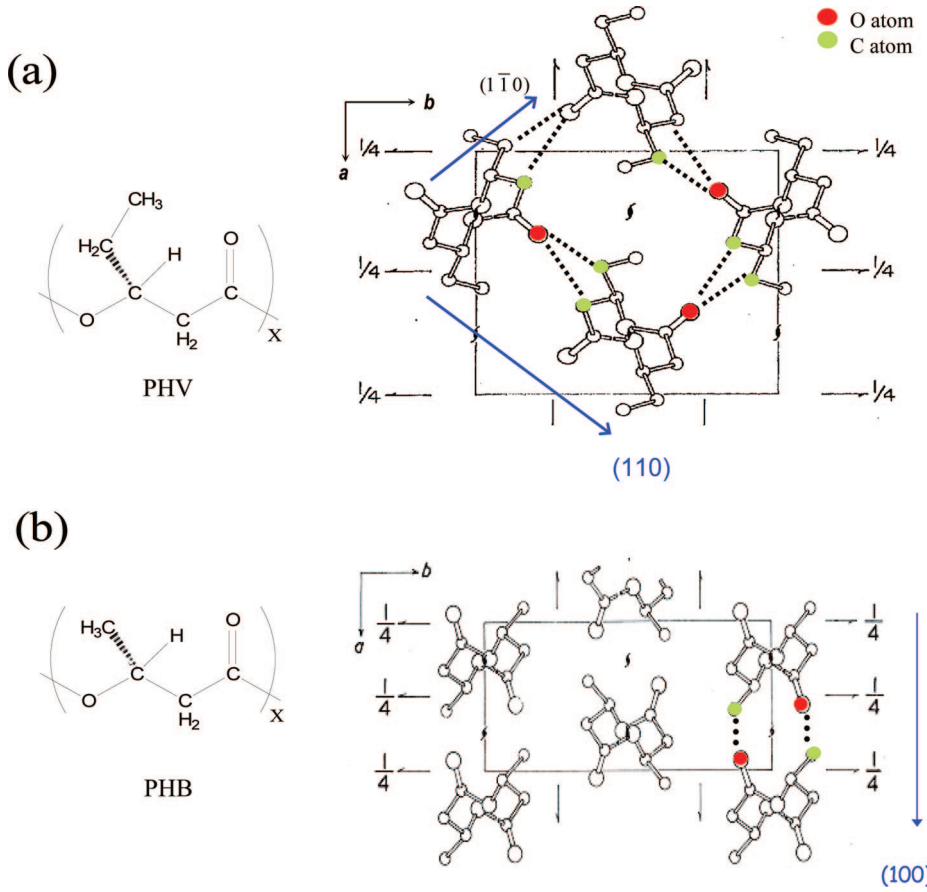

Figure 1. Chemical structures and reported crystalline structures of (a) poly(3-hydroxyvarelate) (PHV) and (b) poly(3-hydroxybutyrate) (PHB). Reproduced with permission from ref 12 (a) and ref 14 (b). Copyright (a) 1974 The Society of Polymer Science, Japan (SPSJ), and (b) 1973 Elsevier Science.

between the 110 and 1$\bar{1}$0 directions.[15] It seems that the C−H···O═C hydrogen bonding stabilizes the chain folding in the lamella structure of PHB and that the high crystallinity partly comes from the C−H···O═C hydrogen bonding.

The purpose of the present study is to investigate the crystal structure, C−H···O═C hydrogen bonding, and thermal behavior of PHV from the functional group level by means of infrared (IR) spectroscopy, wide-angle X-ray diffraction (WAXD), and differential scanning calorimetry (DSC). Since PHV has a longer side chain, its crystallinity may be lower than that of PHB. It might be expected that the thickness of a lamella of PHV is thinner than that of PHB, if the molecular interaction would not be involved in the PHV crystal structure. However, the lamella thickness of PHV is almost the same as that of PHB.[17] Therefore, PHV seems to have also some intermolecular interaction as in the case of PHB. Investigations of the relationship between the hydrogen bonding and its chain folding direction are very important to explore the stabilization of their crystal structures.

Experimental Section

Samples. The bacterial poly(3-hydroxyvarelate) (PHV) sample used in this study was isolated by Fukui et al. from a recombinant *Ralstonia eutropha* harboring the PHA biosynthesis genes of *Aeromoras caviae*.[24] PHB was purchased from Aldrich Corp. and used as is. Films of PHB and PHV were prepared by casting their chloroform solutions on CaF_2 windows. The films were kept in a vacuum-dried oven at 60 °C for 12 h and cooled to room temperature.

Wide-Angle X-ray Diffraction (WAXD). The WAXD data were measured for the solvent-cast samples of PHB and PHV in the scattering angle range of $2\theta = 11.5°-18.5°$ by using a Rigaku RINT2100 X-ray diffractometer equipped with a scintillation detector. Radiation of wavelength 1.5418 Å (Cu Kα) was employed at generator power of 50 kV and 40 mA. The temperature dependence of the WAXD measurement was controlled by using a thermoelectric device (RIGAKU PT30) with an accuracy of ±0.1 °C. The heating and cooling rates were ca. 2 °C/min, and WAXD data were recorded at every 10 °C ranging from 30 to 125 °C for PHV.

IR Measurements. The transmission IR spectra were measured at a 2 cm^{-1} resolution for the cast films of PHV and PHB using a Thermo Nicolet NEXUS 470 Fourier transform IR spectrometer with a liquid-nitrogen-cooled mercury−cadmium−telluride detector. A total of 512 scans were coadded for each IR spectral measurement to ensure a high signal-to-noise ratio. The temperature of the IR cell was controlled by a thermoelectric device (CN4400, OMEGA) with an accuracy of ±0.1 °C. The temperature was increased at a rate of ca. 2 °C /min.

Differential Scanning Calorimetry (DSC). Differential scanning calorimetry (DSC) measurements of PHV and PHB were performed with a Perkin-Elmer Pyris6 DSC under a nitrogen purge over a temperature range from −50 to 160 °C at heating and cooling rate of 2 °C/min. High-purity indium and zinc were used for temperature calibration, and indium standard was used for calibration of the heat of fusion (ΔH). PHV and PHB samples for the DSC measurements were prepared by casting their chloroform solutions on DSC pans.

The rate of temperature increase (ca. 2 °C/min) was the same for the DSC, IR, and WAXD experiments. Before each WAXD and IR measurement, the sample cell was maintained at that temperature for 5 min to make the sample equilibrate. The measuring time for each IR spectrum was about 5−10 min, and that for each WAXD pattern was 30 min. In the cooling process, the temperature was decreased at a rate of ca. 2 °C/min for DSC

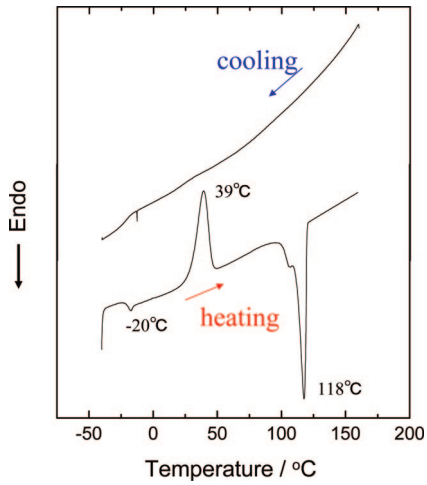

Figure 2. DSC curves of the first cooling run and second heating run of PHV from −50 to 160 °C. Heating and cooling rates of the DSC measurements were 2 °C/min.

while it was decreased at a much slower rate than 2 °C/min for IR and WAXD; the sample was cooled down naturally.

Results and Discussion

Crystal Structures and CH···O═C Hydrogen Bondings of PHV and PHB. Figure 1a,b compares reported crystalline structures of PHV[12] and PHB.[14] Both PHV and PHB have the $P2_12_12_1$ orthorhombic system, and their lattice parameters are $a = 9.32$ Å, $b = 10.02$ Å, $c = 5.56$ Å (fiber axis) for PHV[11,12] and $a = 5.76$ Å, $b = 13.20$ Å, $c = 5.96$ Å (fiber axis) for PHB.[13,14] We previously noticed in the crystal structure of PHB that the CH_3 group in one helix and the C═O group in the other helix are located in the close vicinity along the a axis[18–20] and calculated the distance between the O atom of the C═O group and the H atom of one of the C−H bonds of the CH_3 group from the reported atom coordinates of PHB[14] by using the software QUANTA (Accelrys, San Diego, CA). The atomic coordinates of PHB did not contain those for the H atoms. Therefore, in this calculation, we rotated the CH_3 group to look for the shortest distance between the H atom of the CH_3 group and the O atom of the C═O group. The shortest distance was found to be 2.63 Å.[18–20] The van der Waals separation between the O atom and the H atom is 2.72 Å, and therefore, the distance between the O atom and the H atom in PHB can be significantly shorter than that of the van der Waals separation. The result of this calculation led us to infer the existence of the C−H···O═C interaction in PHB.[18–23]

In the present study similarly, we calculated the shortest distance between the O atom of the C═O group and the H atom of one of the C−H bonds of the two CH_2 groups in PHV, one in the main chain and the other in the side chain. It was found that the shortest distance was found to be 2.38 and 2.61 Å for the main chain and the side chain CH_2 groups, respectively. The distance between the CH_3 and C═O groups is not very short but rather normal for PHV (2.97 Å). Thus, unlike PHB, PHV may have C−H···O═C hydrogen bonding between the C═O group in one helix and one or two CH_2 groups in the other helix. Although the helical structures of PHV and PHB are very similar, their chain folding directions are different: growth planes of PHB single crystals are {100} (along the a axis) while those of PHV are {110}. Different growth directions of PHB and PHV may be concerned with the difference in the CH···O═C hydrogen bondings.

Thermal Analysis. Figure 2 shows the DSC curves of the first cooling and second heating of PHV measured with the 2

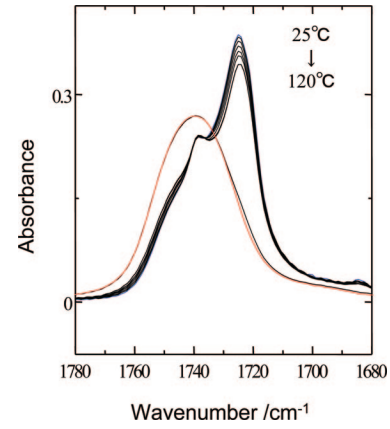

Figure 3. IR spectra in the C═O stretching band region of a film of PHV in the heating process measured over a temperature range of 25−120 °C.

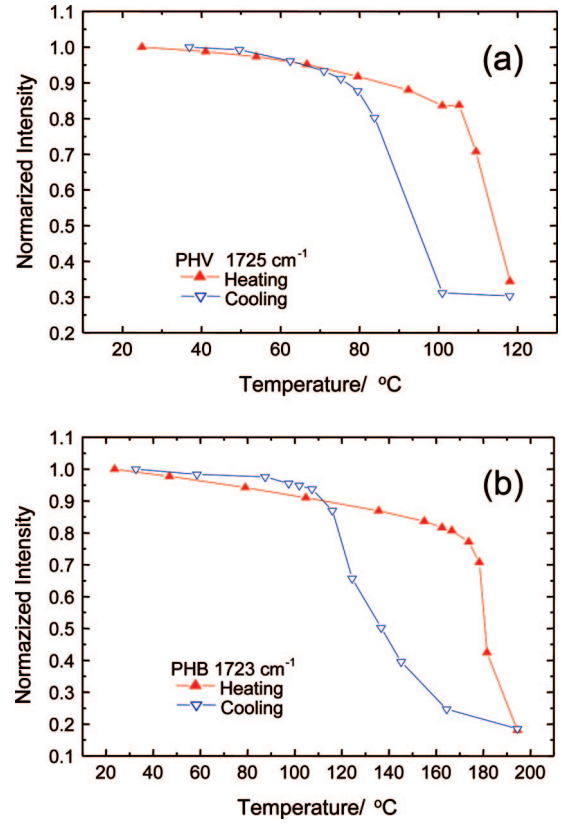

Figure 4. Normalized peak height of (a) the band at 1725 cm^{-1} of PHV and (b) that at 1723 cm^{-1} of PHB vs temperature in the heating and cooling processes.

°C/min. PHV has melting temperature at 118 °C and glass transition temperature of −20 °C. It is noted that the DSC curve of PHV shows a recrystallization process around 39 °C in the second heating run, while PHB has no recrystallization peak in the second heating run at the same heating rate.[18] This means that the crystallization rate of PHV is lower than that of PHB. The calculated crystallinity by using heat of fusion of the DSC curves is 182 J/g for PHB and 103 J/g for PHV. The lower heat of fusion of PHV also shows that PHV has lower crystallinity than that of PHB. It may be expected that comparable values of 100% crystalline heat of fusion for closely related polymers; moreover, the experimentally found difference between heat of fusion of PHB and PHV is very large to be explained only by the differences in the 100% crystalline heat

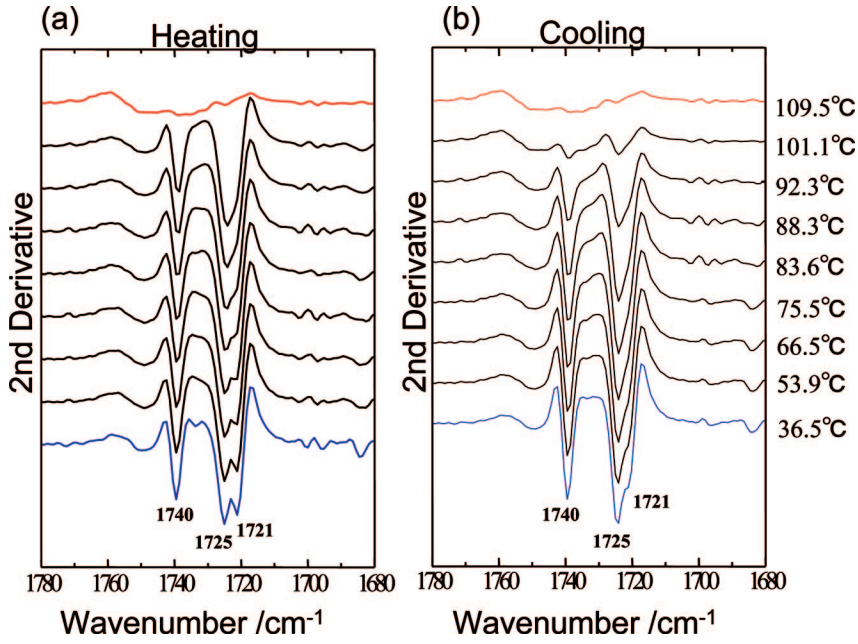

Figure 5. Temperature-dependent variations in the 1780−1680 cm^{-1} region of the second derivatives of IR spectra of the PHB film over a temperature range of 36.5−109.5 °C in the (a) heating and (b) cooling processes.

of fusion. Since PHV has a longer side chain than PHB, it is very likely that the former has lower crystallinity than PHB.

C═O Stretching Band Region of PHV. Figure 3 shows IR spectra in the C═O stretching band region of a film of PHV in the heating process measured over a temperature range of 25−120 °C. Note that there are two bands at 1725 and 1721 cm^{-1} (see the second-derivative spectra in Figure 5) and that the intensities of both bands decrease with temperature increase. In our previous studies of PHB we found similar but single sharper band at 1723 cm^{-1} and assigned it to the C═O stretching band of the crystalline state.[18–23] Therefore, the bands at 1725 and 1721 cm^{-1} of PHV may be due to the C═O stretching modes of the crystalline state. A shoulder near 1740 cm^{-1} seems to contain contributions from both the crystalline and amorphous parts. In the isothermal crystallization experiments at 72 and 90 °C of PHV we found that the intensity at 1740 cm^{-1} increases with time.[23] Thus, the 1740 cm^{-1} band does contain a contribution from the crystalline part. In the spectrum of the amorphous state at 110 °C, a broad feature is observed near 1740 cm^{-1}. This frequency is almost the same as that for the amorphous C═O stretching band of PHB.[18–23] Thus, the 1740 cm^{-1} band also contains the contribution from the C═O stretching mode of the amorphous parts in PHV.

We already reported that the large low-frequency shift of the crystalline C═O stretching band of PHB arises from the formation of C−H···O═C hydrogen bonding between the CH_3 and C═O groups.[18–23] The low-frequency shift of the C═O stretching band and the appearances of the two C═O bands at 1725 and 1721 cm^{-1} suggest that the C═O groups of PHV are involved in some intermolecular interactions with slightly different strength in the crystal structure. It should be kept in mind that the position of the C═O band is related to the strength and not number of hydrogen bonds. The IR results for the C═O stretching bands together with the calculations of the shortest distances between the C═O and CH_2 groups lead us to conclude that there are C−H···O═C hydrogen bondings between the C═O group in one helix and the one or two CH_2 groups in the other helix in PHV. However, even if the C═O groups of PHV have some interaction, not every C═O group seems to be interacting because the spectrum at room temperature shows the free C═O stretching band at 1740 cm^{-1}.

Parts a and b of Figure 4 plot the temperature dependences of the normalized peak height of the C═O stretching band at 1725 cm^{-1} for PHV and that at 1723 cm^{-1} for PHB, respectively. It is noted that the intensities of the C═O stretching bands of PHV and PHB change little until just below their melting points. The thermal behavior of the C═O band of PHV seems to be very similar to that of PHB. This suggests that PHV has some intermolecular interaction like PHB. In the cooling process, the intensity of the C═O band of PHB reaches the maximum around 115 °C, and this is in good agreement with the result of DSC.[24] It seems that the temperature where the highest intensity of the C═O stretching band is reached during the cooling process gives its crystallization temperature. Although PHV does not show the crystallization temperature in the DSC curve because of the different cooling rates in the DSC and FT-IR experiments, the crystallization temperature of PHV is predicted to be about 80 °C from the result of Figure 4a.

Figure 5 shows the second derivatives of IR spectra in the 1780−1680 cm^{-1} region of the PHV film measured in the heating and cooling processes. It can be clearly seen that there are three crystalline C═O stretching bands at 1740, 1725, and 1721 cm^{-1} and that the 1721 cm^{-1} band becomes weaker at the lower temperature than the 1725 cm^{-1} band in the heating process, and it becomes stronger at the lower temperature in the cooling process. These results suggest that there are three kinds of the C═O groups in PHV arising from three different environments in the crystal, although there is only one crystalline form for PHV as is evident from the X-ray diffraction pattern. The 1740 cm^{-1} band arises from the C═O stretching mode of the non-hydrogen-bonding part. The 1725 cm^{-1} band may be due to the C═O stretching mode of the more stable crystalline part which forms the C−H···O═C hydrogen bondings with the two CH_2 groups, one in the main chain and the other in the side chain, while the 1721 cm^{-1} band seems to be ascribed to the C═O group of the less stable crystalline part which forms the C−H···O═C hydrogen bond with one of the two CH_2 groups. It is rather difficult to identify which CH_2 group, that in the side chain or that in the main chain, is concerned with the C−H···O═C hydrogen bonding in the less stable crystalline form.

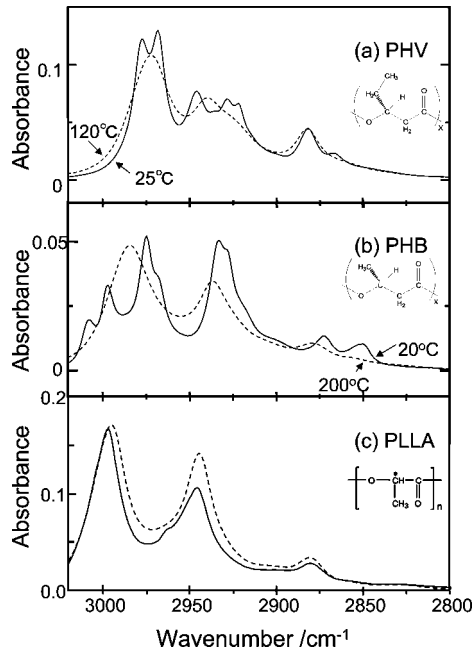

Figure 6. IR spectra in the 3030−2800 cm^{-1} region of (a) PHV and (b) PHB, measured at room temperature (—) and high temperature (above melting point; (a) 118 °C and (b) 176 °C). IR spectra in the same region of PLLA measured during the isothermal melt crystallization at 150 °C: (—) crystalline state and (- - -) amorphous state.

C−H Stretching Band Region of IR Spectra. Weak hydrogen bonds such as C−H···O and C−H···N hydrogen bonds have recently received keen interests, and vibrational spectroscopy and quantum chemical calculations have been used extensively to explore the nature of such weak hydrogen bonds.[25,26] It is well-known that a C−H stretching band of CH_3 or CH_2 group engaging in a C−H···O hydrogen bonding shows a blue shift in an IR or Raman spectrum.[25,26] In our previous studies,[18–23] we concluded on the basis of experimental fact that the C−H stretching band appears at an unusually high frequency (3009 cm^{-1}) and that PHB has a C−H···O═C hydrogen bonding between the CH_3 and C═O groups. A CH_3 asymmetric stretching band usually appears in the 2985−2950 cm^{-1} region. Thus, the appearance of the CH_3 band at 3009 cm^{-1} is a good evidence for the C−H···O═C hydrogen bond.

Parts a, b, and c of Figure 6 compare the C−H stretching band region of IR spectra of PHV, PHB, and poly(L-lactic acid) (PLLA) films at room temperature and high temperature above the melting point, respectively. PHB at room temperature yields a band at 3009 cm^{-1} while PHV does not give a band at such high frequency. This indicates that PHV does not have a C−H···O═C hydrogen bonding between the CH_3 and C═O groups. By comparing the IR spectra of PHV and PHB with that of PLLA, we propose tentative band assignments in the CH stretching region of PHV. PLLA has one CH_3 group and one CH group but no CH_2 group. Thus, it is easy to assign bands at 2997, 2945, and 2880 cm^{-1} bands of PLLA to the CH_3 asymmetric, CH_3 symmetric, and CH stretching modes, respectively (Figure 6c). Thus, two strong features at 2977 and 2968 cm^{-1} of PHV may be assigned to the CH_3 asymmetric stretching modes (Figure 6a). The band assignments in the 2960−2920 cm^{-1} region of PHV are not straightforward because not only CH_3 symmetric band but also CH_2 antisymmetric band appear in this region. We assign a band at 2948 cm^{-1} which shows a low-frequency shift with temperature (see Figure 7) to the CH_2 antisymmetric mode and a pair of bands at 2928 and 2922 cm^{-1} which show little shift to the CH_3 symmetric stretching mode because as in the case of the CH_3 asymmetric bands of PHV it is very unlikely that CH_3 symmetric bands

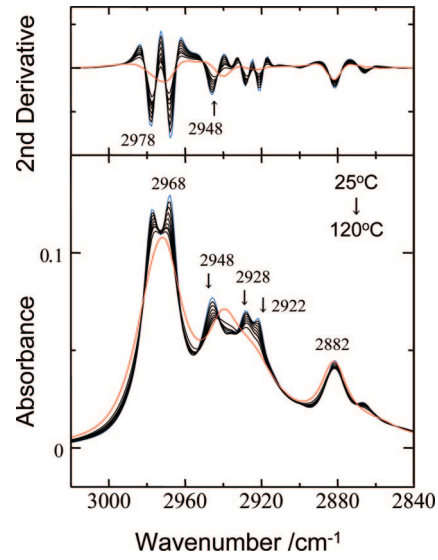

Figure 7. Temperature-dependent variation of the C−H stretching band region of PHV and its second derivative measured over a temperature range of 25 °C (blue line) to 120 °C (red line).

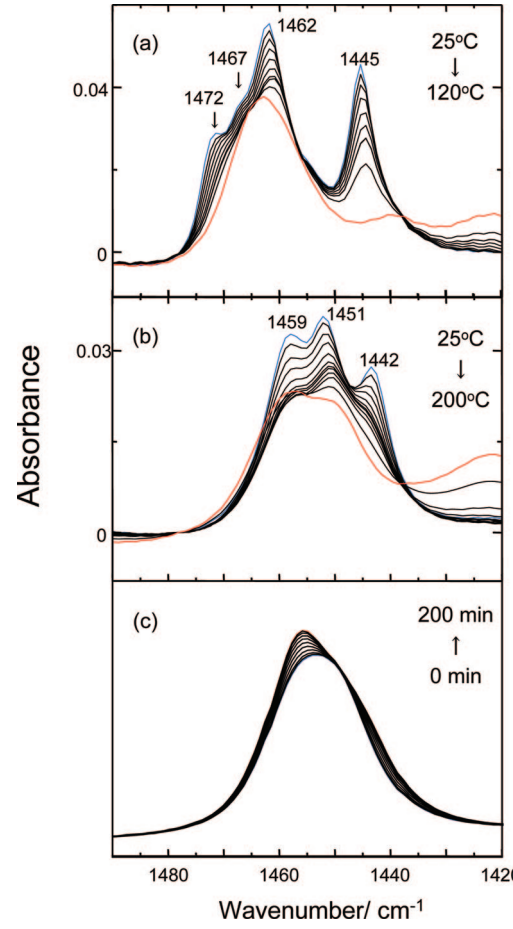

Figure 8. IR spectra in the 1490−1420 cm^{-1} region of (a) PHV and (b) PHB measured in the heating process over a temperature range of (a) 25−120 °C and (b) 25−200 °C (blue line; 25 °C, red line; high temperature). IR spectra in the same region of PLLA measured during the isothermal melt crystallization at 150 °C.

show a shift with temperature increase. A band due to the CH stretching mode of the C−H group is observed near 2880 cm^{-1} commonly in the IR spectra of PHV, PHB, and PLLA (Figure 6a−c). A weak feature near 2870 cm^{-1} of PHV may be attributed to the CH_2 symmetric stretching mode. The corre-

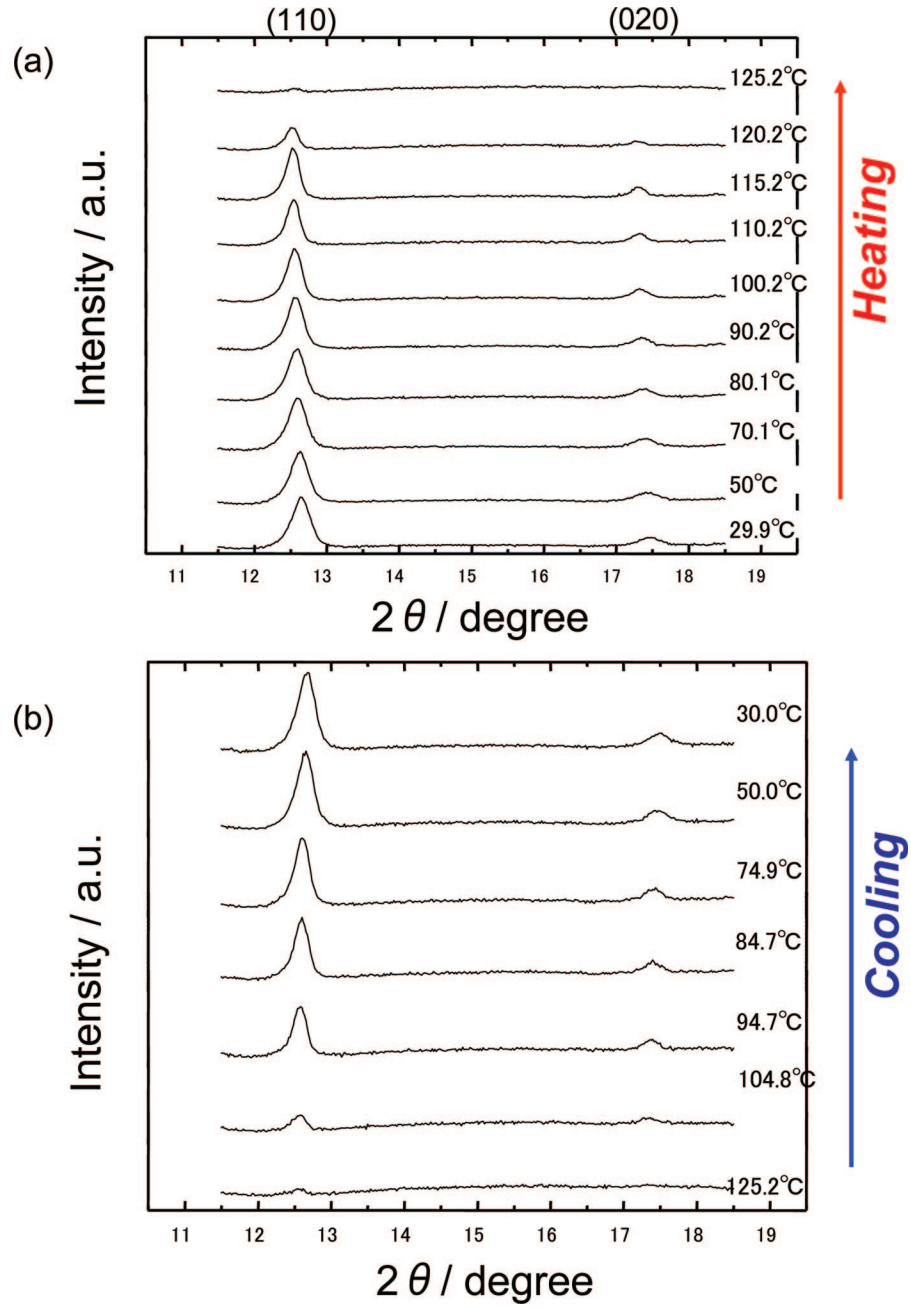

Figure 9. Temperature dependences of the X-ray diffraction of a PHV film measured over a temperature range of 29.9−125.2 °C in the heating process and of 125.2−30.0 °C in the cooling process.

sponding band is, of course, not seen in the spectrum of PLLA but identified near 2850 cm^{-1} in the IR spectrum of PHB. Of particular note is that both CH_2 antisymmetric and symmetric bands of PHV are located at much higher frequencies than at their usual frequencies. The usual frequencies of the CH_2 antisymmetric and symmetric stretching band are 2935−2920 and 2860−2850 cm^{-1}, respectively. These blue shifts of the two CH_2 stretching bands may be good evidence for the formation of the C−H···O═C hydrogen bonds between the CH_2 groups and the C═O group. Figure 7 depicts temperature-dependent variation of the C−H stretching band region of PHV. Note that the CH_2 band at 2948 cm^{-1} becomes weak and shows a low-frequency shift with temperature. This suggests that the C−H···O═C hydrogen bonding becomes weak with temperature.

CH_3, CH_2 Bending Band Region of PHV and PHB. Parts a and b of Figure 8 show IR spectra in the 1490−1420 cm^{-1} region of PHV and PHB measured from 25 °C to their melting temperature, respectively (PHV, 118 °C; PHB, 176 °C). Figure 8c depicts an IR spectrum in the same region of PLLA during the melt crystallization at 150 °C. We again use the PLLA spectrum for band assignment. In the 1490−1420 cm^{-1} region bands due to CH_3 asymmetric deformation mode and CH_2 scissoring mode are expected to appear. PLLA does not have a CH_2 group, so that there is no doubt that a band at 1454 cm^{-1} in the spectrum of PLLA (Figure 8c) is due to the CH_3 asymmetric mode. In this region PHB yields three bands at 1459, 1451, and 1442 cm^{-1} in the spectrum measured at 25 °C and two bands at 1460 and 1449 cm^{-1} in that at 200 °C. It is noted that the band at 1451 cm^{-1} shows a low-frequency shift with temperature while that at 1442 cm^{-1} shows a high-frequency shift. These shifts are small but in parallel with the shift of the 3009 cm^{-1} band, which is due to C−H stretching mode of the C−H(CH_3)···O═C hydrogen bonding.[19,20] Therefore, it is very likely that both the bands at 1451 and 1442 cm^{-1} are assigned to the CH_3 asymmetric bending modes. Since one of the three

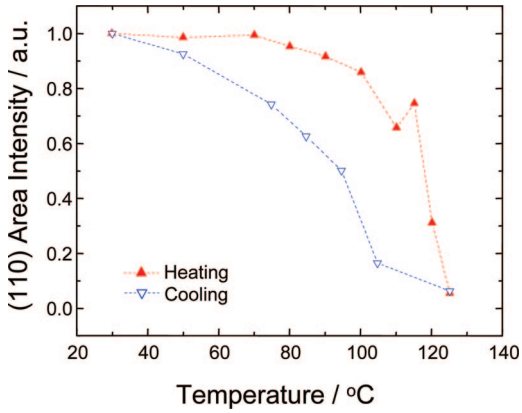

Figure 10. Temperature-dependent variations of the normalized peak area of (110) diffraction of PHV in the heating and cooling processes.

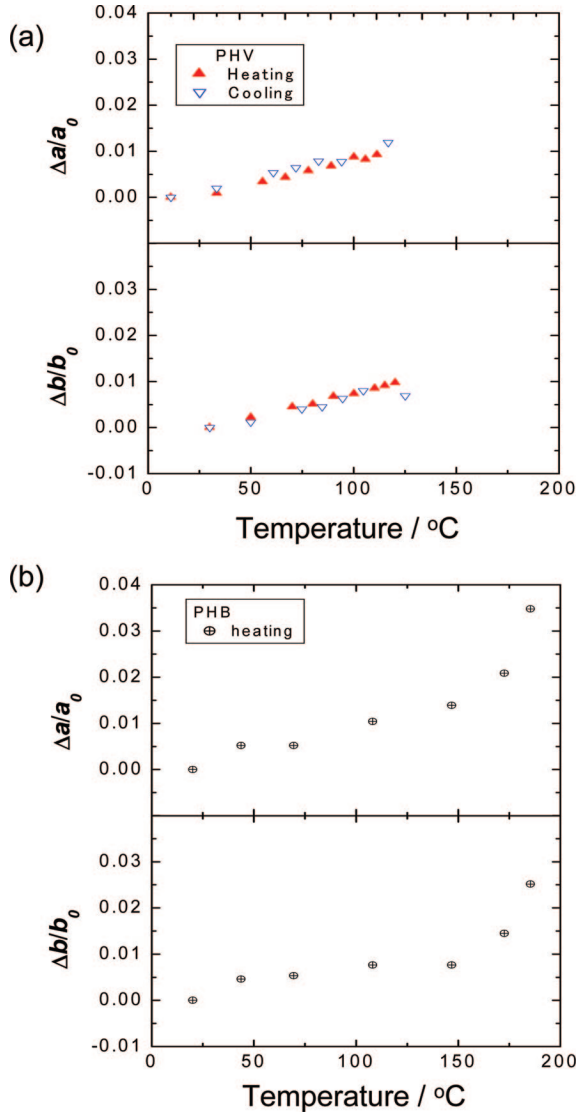

Figure 11. Temperature dependences of (A) $\Delta a/a_0$ and (B) $\Delta b/b_0$ for (a) PHB and (b) PHV. a_0 and b_0 are lattice parameters at 25 °C, and Δa (or Δb) is a difference between a_0 (or b_0) and a (or b), the lattice parameter at a particular temperature.

C−H bonds of the CH_3 group is involved in the hydrogen bonding,[21] it is not a pure CH_3 group but a pseudo-CH_3 group. Thus, the CH_3 asymmetric bending band may be split into two bands. In the spectrum of the amorphous state we observe only one CH_3 band at 1463 cm^{-1}. We assign the band at 1459 cm^{-1} in the PHB spectra to the CH_2 scissoring mode. The CH_2 scissoring band of PHB shifts little with temperature.

Now, we can make band assignments for the PHV spectra. PHV has one CH_3 group and two CH_2 groups, so that the spectra in the 1490−1420 cm^{-1} region are more complicated. They show at least five bands at 1472, 1467, 1462, 1454, and 1445 cm^{-1}. Comparison of the spectrum measured at 25 °C with that at 120 °C reveals that at least the bands at 1472 and 1445 cm^{-1} come from the crystalline parts. It is noted that the 1472 cm^{-1} band shows a gradual low-frequency shift. It may be reasonable to ascribe the band at 1462 cm^{-1} to the CH_3 asymmetric bending mode because it shows only a slight shift with temperature and its frequency is close to that of the CH_3 asymmetric bending band of PLLA.

WAXD Measurements of PHV and PHB. Parts a and b of Figure 9 show the temperature dependences of the WAXD pattern of a PHV film for the heating and cooling processes, respectively. It can be clearly seen from Figure 9 that the (110) and (020) diffraction peaks disappear above its melting temperature (118 °C) during the heating process and that these diffraction peaks appear around its crystallization temperature (80 °C) during the cooling process. Both (110) and (020) peak area intensities indicate the crystallinity of the sample, but we calculated the (110) peak area intensity because the (110) peak is stronger than the (020) peak in Figure 9.

Figure 10 shows the (110) peak area intensity of PHV vs temperature in the heating and cooling processes. This temperature behavior corresponds to that of the normalized peak height of the C═O stretching band at 1725 cm^{-1}, which shows the crystallinity of PHV (Figure 4a). Considering the different conditions of cooling process between the WAXD and FT-IR experiments, both are in good agreement with each other. From the peak positions of (110) and (020), we estimated a and b lattice parameters of PHV. Parts a and b of Figure 11 plot the temperature dependences of $\Delta a/a_0$ and $\Delta b/b_0$ for PHV and PHB, respectively. Here, a_0 and b_0 are lattice parameters at 25 °C and Δa (or Δb) are difference between a_0 (or b_0) and the lattice parameters, a (or b), at the temperature measured. As previously reported,[18] for PHB the a lattice parameter increases much more than the b lattice parameter up to 150 °C. Since in PHB the C−H···O═C hydrogen bonding between the C═O and CH_3 groups exists along the a axis, the a spacing gradually expands with temperature. On the other hand, for PHV both a and b lattice parameters increase similarly with temperature. This may be due to the existence of the C−H···O═C hydrogen bonding along the (110) direction in PHV. The expanding of both lattice parameters indicate that the hydrogen bonding becomes weak and the (110) spacing expands gradually with temperature. The degrees of the changes in the a and b lattice parameter of PHV are smaller than those of PHB.

PHB has a particular C−H···O═C hydrogen bonding between the C═O group and the CH_3 group along the a axis ((110) and ($\bar{1}$10) direction), which is the same direction as its chain folding direction. The difference in the chain folding direction between PHV and PHB may come from the difference in the inter- or intramolecular interactions in their crystal structures.

Conclusions

The present study has aimed at exploring the crystal structure, C−H···O═C hydrogen bondings, and thermal behavior of PHV in comparison with those of PHB. We have reached following conclusions.

1. PHV has C−H···O═C hydrogen bondings between the C═O group in one helix and the CH_2 groups in the main or side chains in the other helix.

2. The C═O groups are in three different environments in the PHV crystal; they are in the more stable part, the less stable part, and the non-hydrogen-bonding part. The former has two C−H···O═C hydrogen bondings with the CH_2 groups in both side and main chains, while the latter has only one C−H···O═C hydrogen bonding with one of the two CH_2 groups.

3. The directions of the C−H···O═C hydrogen bondings are almost in the parallel to the (110) direction, which is the chain folding direction. It is very likely that the C−H···O═C hydrogen bonding stabilizes the chain folding in the lamella structure of PHV.

4. The crystallinity of PHV remains almost unchanged until just below its melting temperature.

Acknowledgment. The authors thank Prof. Isao Takahashi (Kwansei Gakuin University) and Prof. Hiroshi Yamaguchi (Kwansei Gakuin University) for valuable discussions. This work was partially supported by "Open Research Center" project for private universities: matching fund subsidy from MEXT (Ministry of Education, Culture, Sports, Science and Technology), 2001−2008. This work was supported also by Kwansei-Gakuin University "Special Research" project, 2004−2008, Grant-in-Aid for Young Scientists (B) from MEXT (No. 18750107), and 2006 Hyogo Science and Technology Association. Financial support of the Grant Agency of the Czech Republic (project 203/05/0425) is gratefully acknowledged.

References and Notes

(1) Barham, P. J.; Barker, P.; Organ, S. *FEMS Microbiol. Rev.* **1992**, *103*, 289.
(2) Holmes, P. A. In *Developments in Crystalline Polymers*; Bassett, D. C., Ed.; Elsevier: London, 1987; Vol. *2*, p 1.
(3) Lemoigne, M. *Bull. Soc. Chim. Biol.* **1926**, *8*, 770.
(4) Doi, Y. *Microbial Polyesters*; VCH Publishers: New York, 1990.
(5) Vert, M. *Biomacromolecules* **2005**, *6*, 538.
(6) Chiellini, E.; Solaro, R. *Recent Advances in Biodegradable Polymers and Plastics*; Wiley-VCH: Weinheim, 2003.
(7) Bastioli, C. *Handbook of Biodegradable Polymers*; Rapra Technology Limited: Shawbury, 2005.
(8) Iwata, T.; Aoyagi, Y.; Fujita, M.; Yamane, H.; Doi, Y.; Suzuki, Y.; Takeuchi, A.; Uesugi, K. *Macromol. Rapid Commun.* **2004**, *25*, 1100.
(9) Doi, Y.; Kitamura, S.; Abe, H. *Macromolecules* **1995**, *28*, 4822.
(10) Kobayashi, G.; Shiotani, T.; Shima, Y.; Doi, Y. In *Biodegradable Plastics and Polymers*; Doi, Y., Fukuda, K., Eds.; Elsevier: Amsterdam, 1994; p 410.
(11) Marchessault, R. H.; Debzi, E. M.; Revol, J. F.; Steinbuhel, A. *Can. J. Microbiol.* **1995**, *41*, 287.
(12) Yokouchi, M.; Chatani, Y.; Tadokoro, H.; Tani, H. *Polym. J.* **1974**, *6*, 248.
(13) Cornibert, J.; Marchessault, R. H. *J. Mol. Biol.* **1972**, *71*, 735.
(14) Yokouchi, M.; Chatani, Y.; Tadokoro, H.; Teranishi, K.; Tani, H. *Polymer* **1973**, *14*, 267.
(15) Marchessault, R. H.; Kawada, J. *Macromolecules* **2004**, *37*, 7418.
(16) Marchessault, R. H.; Yu, G. In *Biopolymers, Polyesters II*; Doi, Y., Steinbüchel, A., Eds.; Wiley-VCH: Wienhiem, 2002; p 157.
(17) Iwata, T.; Doi, Y. *Macromolecules* **2000**, *33*, 5559.
(18) Sato, H.; Nakamura, M.; Padermshoke, A.; Yamaguchi, H.; Terauchi, H.; Ekgasit, S.; Noda, I.; Ozaki, Y. *Macromolecules* **2004**, *37*, 3763.
(19) Sato, H.; Murakami, R.; Padermshoke, A.; Hirose, F.; Senda, K.; Noda, I.; Ozaki, Y. *Macromolecules* **2004**, *37*, 7203.
(20) Sato, H.; Dybal, J.; Murakami, R.; Noda, I.; Ozaki, Y. *J. Mol. Struct.* **2005**, *744–747*, 35.
(21) Sato, H.; Mori, K.; Murakami, R.; Ando, Y.; Takahashi, I.; Zhang, J.; Terauchi, H.; Hirose, F.; Senda, K.; Tashiro, K.; Noda, I.; Ozaki, Y. *Macromolecules* **2006**, *39*, 1525.
(22) Zhang, J.; Sato, H.; Tsuji, H.; Noda, I.; Ozaki, Y. *J. Mol. Struct.* **2005**, *249*, 735–736.
(23) Hu, Y.; Zhang, J.; Sato, H.; Futami, Y.; Noda, I.; Ozaki, Y. *Macromolecules* **2006**, *39*, 3841.
(24) Fukui, T.; Kichise, T.; Yoshida, Y.; Doi, Y. *Biotechnol. Lett.* **1997**, *19*, 1093.
(25) Desiraju, G. R.; Steiner, T. The Weak Hydrogen Bond. In *Structural Chemistry and Biology*; Oxford University Press: Oxford, 1999; pp 29−121.
(26) Matsuura, H.; Yoshida, H.; Hieda, M.; Yamanaka, S.; Harada, T.; Shinya, K.; Ohno, K. *J. Am. Chem. Soc.* **2003**, *125*, 13910.

MA702222A